HHS Public Access

Author manuscript

Dev Biol. Author manuscript; available in PMC 2023 July 13.

Published in final edited form as:

Dev Biol. 2022 November ; 491: 56–65. doi:10.1016/j.ydbio.2022.08.005.

Wound repair in sea urchin larvae involves pigment cells and blastocoelar cells

Raymond L. Allen[2,4],

Andrew N. George[3,4],

Esther Miranda[1],

Taji M. Phillips[1],

Janice M. Crawford[1],

Daniel P. Kiehart[1],

David R. McClay[1,*]

Department of Biology, Duke University, Durham NC 27708

Abstract

Sea urchin larvae spend weeks to months feeding on plankton prior to metamorphosis. When handled in the laboratory they are easily injured, suggesting that in the plankton they are injured with some frequency. Fortunately, larval wounds are repaired through an efficient wound response with mesenchymal pigment cells and blastocoelar cells assisting as the epithelium closes. Within seconds of an induced wound a calcium transient, initiated by the wound, rapidly spreads around the entire larva and is necessary for activating pigment cell migration toward the wound. If calcium transport is blocked, the pigment cells fail to activate and remain in place. When activated, pigment cells immediately initiate directed migration to the wound site from distances of at least 85μm. Upon arrival at the wound site they participate in an innate immune response. Blastocoelar cells are recruited to the injury site as well, though the calcium transient is unnecessary for activating these cells. At the wound site, blastocoelar cells participate in several functions including remodeling the skeleton if it protrudes through the epithelium.

Keywords

Larval wound repair; skeletal remodeling; pigment cell motility

Introduction

Echinoderms live in an ocean environment rich with bacteria and viruses. To protect themselves, these animals have evolved an efficient innate immune system that is present throughout the life history of the animal (Smith et al., 2010). This includes protection of

*Address for correspondence: David R. McClay, Department of Biology, Duke University, Box 90338, Durham, NC 27707, Phone: 919-613-8188, dmcclay@duke.edu.

[1]Current address: Department of Biology, Duke University, Box 90338, Durham, NC 27708

[2]Current address: Center for Limnology, University of Wisconsin-Madison, 3110 Trout Lake Station Dr, Boulder Junction, WI 54512

[3]Current address: North Carolina Biotechnology Center, 15 T.W. Alexander Dr., Research Triangle Park, NC 27709-3547

[4]Co-first authors

the larvae as they feed and grow in the water column for up to several months before undergoing metamorphosis. The larval stage is reached within a few days after fertilization and as soon as they reach that stage, larvae are armed with the ability to fight infections (Ch Ho et al., 2016). Several immune cell types found in the blastocoel are collectively referred to as “blastocoelar” cells. These differ morphologically, though their functional differences are not known (Ch Ho et al., 2016). Another immune cell type, pigment cells, differentiate within the blastocoel next to the dorsal epithelium while other pigment cells move into the dorsal epithelium of the larva. In healthy larvae these cells constantly move, likely conducting immunosurveillance in much the same way dendritic cells move within the epithelium of vertebrates.

As larvae feed, they ingest pathogenic bacteria and viruses, and in response both blastocoelar cells and pigment cells move to the gut (Buckley et al., 2017; Buckley and Rast, 2015, 2019; Buckley et al., 2019; Ch Ho et al., 2016; Smith et al., 2010). When handling the larvae in the laboratory, they are easily injured especially from wounds incurred by the penetration of the sharp tips of the larval skeleton through the epithelium from the inside. Observation of those wounds over time suggests that repair is relatively rapid. When followed closely, both pigment cells and blastocoelar cells respond by moving to the site where they assist in the response. That response is the subject of this study.

The cell biology of the echinoderm immune system began about 140 years ago when Metchnikoff pierced a starfish larva with a tangerine thorn and noticed that over time cells gathered on the inserted thorn (Gordon, 2016). Those cells were undoubtedly blastocoelar cells, and were part of Metchnikoff’s discovery of innate immunity. Modern research on the innate immune system in sea urchin larvae has focused primarily on the molecular apparatus used in response to an infection, with orthologs to vertebrate immune response genes as the major focus of molecular discovery (Buckley et al., 2017; Buckley and Rast, 2012, 2015; Rast et al., 2006), and more recently, the microbiome (Carrier et al., 2021; Fleming et al., 2021). Pigment cells provide immune protection through exocytosis of intracellular vesicles containing echinochrome A, a pigment shown to have both bactericidal and antiviral activities (Coates et al., 2018; Fedoreyev et al., 2018; Service and Wardlaw, 1984). Blastocoelar cells express a number of Toll-like receptors, cytokines and other molecules known to be involved in immune responses (Buckley and Rast, 2012, 2015; Rast et al., 2006). Although the genome has revealed the presence of a number of additional immune candidate genes, little is known about how blastocoelar and pigment cells detect pathogens, and become activated to respond. In the laboratory pigment cells and blastocoelar cells briskly respond to an injury even though relatively low numbers of bacteria are present.

Blastocoelar cells and pigment cells are derived embryonically from non-skeletal mesenchyme (NSM). The NSM gene regulatory network (GRN) is activated by Delta-Notch signaling beginning at 5^{th} cleavage (Sweet et al., 2002). Delta, expressed by micromeres, activates the Notch receptor on adjacent macromeres (Sherwood and McClay, 1997, 1999). Notch signaling activates expression of *gcm*, an upstream transcription factor in the mesoderm GRN (Ransick and Davidson, 2006, 2012). NSM cells expressing *gcm* initially form a ring of cells that surround the micromeres at the vegetal pole of the embryo. At hatching, a Nodal signal from the ventral ectoderm leads to loss of *gcm* expression on the

ventral side of the NSM, while *gcm* persists in the dorsal NSM (Duboc et al., 2010). The dorsal *gcm*-expressing cells become the progenitors of the pigment cells. Two markers of the pigment cell lineage are *pks1* (polyketide synthase 1), an enzyme in the pathway leading to production of echinochrome A, and *sult* (sulfotransferase) (Calestani et al., 2003; Calestani and Wessel, 2018). *Sult* and *Pks1* are used here as *in situ* hybridization markers of pigment cell progenitors. These become specific to pigment cell progenitors after the mesenchyme blastula stage. The echinochrome A pigment is first visualized in pigment cells at the early pluteus stage when the remaining enzymes in the echinochrome pathway are present.

Early in gastrulation pigment cell progenitors move to, and invade the dorsal ectoderm by passing through the basement membrane. In some way this process involves specific ephrin-eph recognition (Krupke et al., 2016), because inhibition of that pathway results in ectopic epithelial entry. Once in the dorsal ectoderm the pigment cells spread out and conduct immunosurveillance with an ability to respond to infections in the epithelium and gut (Buckley and Rast, 2019). Some pigment cells remain in the blastocoel and migrate along the lining of the dorsal blastocoel.

Blastocoelar cells originate from ventral NSM cells. These cells extinguish *gcm* expression in response to Nodal signaling. Most blastocoelar cells undergo an epithelial to mesenchyme transition (EMT) as the archenteron completes invagination, though a few may leave the archenteron earlier. Once in the blastocoel, some of these cells populate the extracellular matrix throughout the blastocoel while many others remain motile, and in the process actively extend a rich network of filopodia (Miller et al., 1995; Buckley et al., 2017; Tamboline and Burke, 1992). Migratory blastocoelar cells are interpreted as being active in immunosurveillance while substrate-bound blastocoelar cells are thought to be activated only during an immune response (Ch Ho et al., 2016).

Here we report on cell biological functions of pigment cells and blastocoelar cells in wound repair. Pigment cells are activated by calcium and are recruited to the site of the wound where they release echinochrome A as part of an immune reaction. Blastocoelar cells also participate in the wound response, surprisingly as participants in the remodeling of the skeleton.

Results

Pigment cells reach the dorsal ectoderm via an EMT followed by re-entry into the dorsal epithelium.

During gastrulation, pigment cell progenitors leave the blastoderm using an EMT. In *Lytechinus variegatus (Lv),* this occurs at the end of the mesenchyme blastula stage and is coincident with the onset of archenteron invagination (Fig. 1A–C). This places the pigment cell progenitors next to the ring of recently ingressed skeletogenic cells. From there, most pigment cell progenitors move to the dorsal posterior ectoderm where many of them enter the epithelium of the dorsal ectoderm (Fig. 1D–I). Once in the dorsal epithelium, pigment cell progenitors move within the plane of the epithelium toward the anterior as tracked over time using expression of *sult* (sulfotransferase) (Calestani et al., 2003) as a pigment cell-specific *in situ* marker (Fig. 1A–C). During this transit the number of pigment cells

roughly doubles. Pigment cells were counted in 5 embryos per time point between 11 hpf (before the EMT begins), to 17 hpf, when gastrulation is completed. By that time pigment cell progenitors reach the anterior extent of the dorsal ectoderm. Fig. S1 shows the increase in pigment cell number, as well as their location over time, and suggests that most of the cell divisions occur after the progenitors complete EMT. The cells divide asynchronously about one time (on average). At 11 hpf, prior to pigment cell EMT, about 25 cells are positive for *sult* expression per embryo and by the end of gastrulation there are about 50 *sult*-expressing cells, though the absolute number of pigment cells varies from batch to batch suggesting there is a genetic component contributing to pigment cell number. After entering the dorsal epithelium and migrating anteriorly, pigment cell progenitors space themselves relatively uniformly through movements that appear random. Pigment cells on the lining of the blastocoel also migrate anteriorly and tend to remain on the lining of the dorsal ectoderm. Later, at prism to early larval stage, the pigment cells differentiate, express echinochrome A, and are observed to be scattered throughout the dorsal epithelium and along the dorsal lining of the blastocoel.

Expression of echinochrome A allows pigment cells to be easily distinguished in an otherwise transparent larva, so most experiments from differentiation onward followed pigment cell behavior in 576 movies by time-lapse. Data from those movies is distilled in the results that follow. Movie S1 shows the motile behavior of the pigment cells over time as they move in a healthy embryo. As can be seen, the pigment cells in the body of the larva move in seemingly random directions and directional changes occur frequently. About 46 uninjured embryos were recorded. Fig. S2A shows traces of one such time-lapse movie. Cells moved in and out of focus in this movie, and the trace for each cell shows that they move but tend to remain local relative to their starting position. Processes from one pigment cell frequently touch another pigment cell when they come into close proximity (Movie S1). That touch-direction change may contribute to the spacing mechanism. Over time, this simple strategy could at least partially account for maintenance of the spacing. Pigment cells were quantified for distances moved over time in 5 healthy larvae. The speed and distances moved in the larva are displayed in Fig. S2B. In both the arms and in the body of the embryo, pigment cells located in the epithelium moved slowly and with a modest displacement. Pigment cells in the blastocoel however, moved faster and with a greater displacement in the body relative to the arms. The blastocoelar space in the arms is small relative to the space in the body, likely accounting for the difference. (Fig. S2B). A separate analysis tracked total distance traveled and total displacement from the starting location of all pigment cells in 6 control embryos over three hours. Those data revealed that on average pigment cells in the arms move a measured total of 53 μm/hr with a total displacement from origin of about 20 μm over those three hrs. In the body the total movement of all pigment cells was an average of 79 μm/hr with a large variation of distance traveled from 40 to 120 μm for different cells, in agreement with the data shown in Fig. S2B. The total displacement of body cells averaged about 30 μm over those three hrs, again indicating that on average, body pigment cells migrate farther than pigment cells in the arms, but still remain relatively confined to a localized area. These measurements change dramatically when the larva is wounded.

The immune response of pigment cells.—The response of pigment cells to a pathological bacterial challenge was tested first. Bacteria from an infection known as “bald sea urchin disease” (Becker et al., 2008), on the surface of an adult sea urchin, were added to cultures of 24 hpf larvae and cultured for an additional 24 hrs (see methods). Control cultures were healthy and active for more than three days. After 12 hrs larvae in the diseased culture began to stop swimming, fell to the bottom of the dish, and displayed a progressive series of changes. In some cases we captured movies of pigment cells swarming to the site of an infection (Movie S2). We examined larvae periodically during the day. The typical progression of the disease began with the swarming of pigment cells and over time pigment cells turned dark red, then black, and degranulated, then seemed to disappear without pigment to identify them (Fig. 2). The larvae also ingested bacteria and in response under the pathogenic condition, pigment cells accumulated on the surface of the gut as reported previously (Ch Ho et al., 2016), and they released echinochrome A turning the gut red. In these infections the larvae eventually die and as they approach death the pigment cell population is greatly reduced. The few remaining pigment cells in Fig. 2 have turned black.

Under normal culture conditions (and probably in the ocean), larvae survive and swim in sea water with what must normally be a lower concentration of pathogenic bacteria. Nevertheless, the larvae survive in ocean water that is rich in bacteria. Most animals, including these larvae, employ the epithelial layer as their primary organ of defense against infection. When the epithelium is penetrated the animal becomes susceptible to infection, so we next asked how the larva responds when a wound is introduced. The sharp tips of larval skeletons easily penetrate through the epithelium. That penetration provides an entry location for an infection, so we focused on that puncture wound as an assay for following the course of an infection.

Both pigment cells and blastocoelar cells contribute to wound repair.—A simple bioassay was developed by forcing skeletal tips to penetrate through the epithelium from the inside (see methods). Movies of 250 larvae, most of them 48 hpf larvae, each with penetrating skeletal tips, were assayed. Movies S3 and S4 illustrate the dynamics observed in those movies. The following was seen during the 60–120 min following an introduced skeletal tip injury, (1) pigment cells rapidly and directionally migrate to the site of the injury starting immediately after introduction of the wound, (2) blastocoelar cells migrate to the site of the wound and penetrate into and through the epithelium, (3) lamellipodia from a blastocoelar cell wrap around the externalized skeletal tip, (4) often the tip of puncturing skeletal rod is degraded and broken, (5) pigment cells at the site of the wound degranulate, and (6) the epithelium migrates to cover the skeletal rod stumps and close the wound. These responses were most common though there was some variation; *e.g.* the excision of the skeletal rod is not always completed in the 60–120 min. sequence, or the epithelium moves to cover the penetrating skeletal tip before it breaks. Below we detail these observations and experiment to learn how the process works.

Pigment cells migrate to the wound site.—Pigment cell behavior was tracked and quantified using MtrackJ in Image J (Fig. 3). A total of fifteen movies were tracked. Although there were minor differences in number of pigment cells responding, distance

traveled, speed range, directional changes, the 15 movies were very similar. Fig. 3 reports on one of the movies to summarize the behavior and measurements seen in all of the movies. Over the first 10 min the pigment cells that were tracked move directionally toward the site of the closest injury in the oral hood of the larva. Quantification provided several insights. Pigment cells were already moving toward the nearest injury at the start of the imaging (about 1–2 min. elapses between the wound and the start of the time-lapse sequence in the mechanical wound assay). Tracking was done by locating the pigment cells in a Z-stack of images collected at each 30 sec interval, then tracking the pigment cells through the Z-stack sections over time, and finally each 10 min interval was compressed to a single two-dimensional image. Cells closest to the injury are the first to move followed by cells farther away from the wound site. In comparing the red, green and purple cells in Fig. 3, by 10 min the red cell, starting about 50 μm from the left injury, had moved over 40 μm toward the injury, the green cell, starting 50 μm from the injury, had moved about 20 μm away from the injury, and the purple cell, starting at about 85 μm distant had hardly moved. Ten min later the green cell reversed course and joined the red cells trajectory toward the injury, however their speed decreased from about 4 μm/min to about 2 μm/min. The purple cell begins to move between 10 and 20 min. post injury and it moves at the slower 2 μm/min rate toward the site of wound. The yellow, blue and orange cells toward the right side of the oral hood have similar velocities toward the injury on the right side with the fastest movement recorded by the closer yellow and blue cells during the first 10 min., followed by the more distant orange cell beginning at 20 min post injury at the slower rate per min. The movement of the red cell toward the left side is particularly informative. Initially it is located 50 μm from the left side and 70 μm from the right. It moves toward the closest site. At first, however, the red cell is biased not directly toward the left injury site but perhaps is influenced weakly by the right side. All other cells similarly move toward the site of the closest injury. The yellow and blue cells reach the injury site by 20 min and their movement then becomes entirely local. The blue cell provides additional information as it is in focus in all four panels. In the last two images the blue cell is observed to separate into a stellate shape, a property that occurs when pigment cell filopodia redistribute echinochrome A-containing granules to spread out the cell (Ch Ho et al., 2016). At higher magnification, the pigment cells degranulate in response to bacterial infections (Ch Ho et al., 2016), and become largely transparent. Thus, upon injury, distant pigment cells rapidly increase their motility in a directional trajectory toward the site of the injury. One reason for the difference in speed of the responding pigment cells is that pigment cells within the blastocoel move with the highest rate of speed while the cells within the epithelium move more slowly. The rapid initiation of the response tends to rule out induced secretion of cytokines and favors rapid responses such as introduction of calcium at the wound site as a possible candidate for initiating the movement. The persistence of a directed movement over time, however, may be a different signal. This raised the question about how the response is initiated.

A calcium transient occurs immediately in response to a wound.—We adapted our assay to a laser imaging system (see methods). From the perturbations described above, we knew that distant pigment cells initiated their directed movements very shortly after an injury. Blastocoelar cells also responded quite rapidly. Given the rapid response we hypothesized that a calcium transient was introduced by cellular or intraembryonic exposure

to sea water. To test this hypothesis, Calcein Green Dextran (CGD), a dye that fluoresces upon increased calcium concentration, was injected into the eggs at fertilization (Covian-Nares et al., 2010). Fig 4 and movie S5 show the response. Control embryos were mounted on a slide with care to avoid injury. The microscope was focused on the plane of the dorsal epithelium. The imaging system was switched to a high-speed camera system that captures fluorescent light. A pre-programmed laser cut was introduced along a designated line of the epithelium. As seen in movie S5 the laser wound is accompanied by fluorescence as the laser cuts in a line through the epithelial cells. That was expected since the laser-damaged cells are exposed to 3mM Ca^{++} in the sea water. Normally the epithelial cell cytoplasm is orders of magnitude lower in Ca^{++} concentration. Immediately thereafter, a wave of fluorescence spreads across the adjacent un-injured epithelium over the next several seconds (Movie S5). Fig. 4A–D. Shows four frames of that movie pseudocolored to provide a heatmap of the response. Within five seconds the entire surface epithelium in focus exhibits the fluorescent flash. The rate of speed of the fluorescent wave roughly approximates the speed of fast calcium waves previously recorded in the sea urchin embryo (Eisen et al., 1984; Jaffe, 1991; Jaffe and Creton, 1998). This indicates that a likely membrane depolarization causes the opening of rapidly responding calcium channels or gap junctions. Thus, a calcium transient is introduced by the wound. But do the pigment cells use that transient to initiate their movement toward the wound site?

To address that question we repeated the laser wound, this time in the presence of verapamil, a calcium channel inhibitor. A wound was introduced by the laser 30 min after larvae were placed in verapamil (50 μm). The cells wounded by the laser cut fluoresced, but after the cut there was no membrane spread of fluorescence (Movie S6, Fig. 4E–H). The wound was repeated using the standard bioassay in which a mechanical injury was introduced. In the seconds and minutes that followed, the pigment cells failed to initiate their directed movement toward the penetrating skeletal tips (Movie S7). This indicated that the calcium transient in some way activates the pigment cells to initiate their movement. Propagation of the transient requires active calcium channels that are inhibited by verapamil. Though pigment cells failed to move in the verapamil-inhibited larvae, some blastocoelar cells (transparent cells in the movie) continued to move suggesting that these cells initiate a response to the wound by a mechanism that is different from the pigment cells.

Wound repair occurs in the absence of pigment cells.—The movies showed that responding pigment cells often degranulate at or near the site of the injury. While this suggested they were active in an immune response, we wondered to what extent the pigment cells participated in wound repair and did they participate in the degradation of the skeleton? These questions were approached in two ways. First, morpholinos were used to knock out pigment cells. As discussed in the introduction, *gcm,* an early-expressed mesoderm transcription factor, is necessary for specification of pigment cells (Ransick and Davidson, 2006, 2012). When *gcm* expression is knocked down, larvae are albino, yet wound healing remains robust. Fifty-five movies were made of larvae that had been injected with a concentration of *gcm* morpholino that results in albino but otherwise normal-looking larvae. Fig. 5 and movie S8 show the wound response which includes a sudden loss of the skeletal tip and closure of the epithelium. Thus, while pigment cells move to the site of the

injury, become stellate and often degranulate to release echinochrome A as a bactericide (Service and Wardlaw, 1984), other cells also participate in the wound repair, including the broken skeletal tip response.

Blastocoelar mesenchyme populations respond to the skeletal-epidermal injury by remodeling the skeleton.—About 20% of the 350 movies reviewed (mechanically wounded and albino mechanically wounded), included excision of a skeletal rod tip (movies S4 and S8), and pigment cells were not necessarily present for that excision. A number of the movies showed very active transparent cells to exit the epithelium and wrap themselves around the skeletal rod. In many of those cases the skeletal rod tip breaks at the site of the wrapping cell. The tip, if outside the embryo, is usually lost, but if retained by the embryo, movie sequences showed it to be resorbed. We hypothesized that the wrapping cells are blastocoelar cells.

To test this hypothesis, we reasoned that the wrapping cells were either epithelial cells or blastocoelar cells. If they were epithelial they should originate locally, but if they were blastocoelar cells, some would originate at a distance from the wound. To test this hypothesis, we injected half or ¼ of the embryo at the 2- or 4-cell stage with mRNA consisting of *gfp* coupled to a transmembrane sequence (Saunders and McClay, 2014). This results in cells of half or a fourth of the larva to be fluorescent. If the hypothesis were supported, we expected to see, with some frequency, GFP-fluorescent cells wrapping around skeletons on the uninjected side of the embryo, an outcome that could only happen if the responding cells migrated from the injected side of the embryo. Fig. 6 and movie S9 shows such a sequence indicating that the cells remodeling the skeleton are not from the local epithelium, and likely are blastocoelar cells. In the movie the fluorescent cell dynamically moves around a protruding skeletal tip just as we observed in a number of movies where the skeletal tip disappeared. The left postoral arm in movie S9 is unlabeled with fluorescence. It is outlined in Fig. 6A. The dynamic fluorescent wrapping cell shown in movie S9 and in Fig. 6B–E had to come from elsewhere, supporting the hypothesis that the cell cutting the skeletal tip is a blastocoelar cell.

As a control for the assignment of blastocoelar cells as the skeletal cutters, we eliminated some classes of blastocoelar cells, but retained pigment cells, and asked what properties of the injury response were retained. Many (but not all) blastocoelar cells express *irf4,* a transcription factor that in the mammalian immune system is expressed by dendritic cells, among others. (Biswas et al., 2010; Bollig et al., 2012; Flutter and Nestle, 2013; Pohl et al., 2017; Tussiwand et al., 2012; Williams et al., 2013). Morpholino knockdown of *irf4* eliminates most blastocoelar cells as indicated by absence of blastocoelar cell markers (*astacin4* and *ron*, Fig. 7 E–H), whose expression is controlled directly or indirectly by Irf4. Without *irf4* expression, we also observed an augmented number of pigment cells (Fig. 7C,D). As above, about 20% of control movies over a 2 hr period lose a skeletal tip to excision. Given that, in the 31 movies of *irf4* knockdown larvae, we should have seen about six that exhibit excision. We saw none, suggesting that blastocoelar cells expressing *Irf4* were responsible for the skeletal excisions.

Discussion

Pigment cells and blastocoelar cells are two of the several cell types in the sea urchin larva that are derivatives of the non-skeletal mesoderm lineage (muscle cells and coelomic pouch cells also originate from this lineage). Skeletogenic cells undergo an EMT at about 9 hpf. Pigment cells leave the blastoderm by way of an EMT at about 12 hpf, the blastocoelar cells enter the blastocoel via an EMT at about 16 hpf. Pigment cells in other species have been reported to ingress prior to, (as seen in *Lv*), or during archenteron invagination (Gibson and Burke, 1985; Gustafson and Kinnander, 1956; Kominami et al., 2001). Many of those earlier observations were made prior to the availability of markers for the pigment cell progenitors and blastocoelar cell progenitors so the timing in other species may need to be revisited. In *Lv*, the lineage markers allow the investigator to follow the spatial trajectory of each of the mesodermal cell types as they undergo morphogenesis, and in the pigment progenitors, prior to production of pigment.

Pigment cells and blastocoelar cells respond to an injury, and participate in the wound repair of sea urchin larvae. After their epithelial-mesenchyme transition, both cell types move to the sites in the embryo where they differentiate and begin to engage in immunosurveillance. The pigment cells normally conduct their immunosurveillance by random movements in and just beneath the epithelium. Their behavior includes contact with nearby pigment cells which is brief and may account for the frequent changes in direction of movement. Upon injury the pigment cells respond almost immediately. Evidence indicates that a rapidly spreading Calcium transient somehow activates the pigment cells. Within seconds of an injury the pigment cells begin a rapid movement toward the injury site. How calcium leads to activation the pigment cells is not known, nor is Calcium likely to be the directional signal used by the pigment cells in their movement toward the injury site. The diffusion of the calcium ion is too rapid and lacks the persistence necessary to explain movement toward the wound site for 30 min or more. But, the fact that the movement is persistent and directional suggests that at least one additional molecule is involved, likely producing a gradient of attraction. The calcium transient appears not to affect blastocoelar cells because they continue their movement in the presence of the calcium inhibitor while the pigment cells remain relatively silenced.

Movement of cells to the wound site initially is rapid with the closest pigment cells responding first. Movement toward the wound slows with time after the wound is initiated. This decrease in rate of movement toward the wound could be due to a decrease in the concentration of the attraction signal, assuming there is such a signal, but until a signal is identified, the parameters surrounding rate of movement remain speculative. When there are two wounds in different regions of the embryo a pigment cell moves toward the closest wound suggesting a stronger attractive signal. Pigment cells lining the blastocoel move to the wound site more rapidly than pigment cells embedded in the epithelium. Since the pigment cells in the blastocoel move directionally in a fluid-filled compartment, the attraction signal must somehow provide directionality in that fluid environment. Blastocoelar cells also respond and move toward the wound though less is known about their migration since they are transparent making them difficult to follow. At least some of them

are able to migrate to the wound from some distance as demonstrated by the fluorescent labeling experiment.

The dynamic movements of pigment cells at the site of the wound includes passage to or from the epithelium either into the blastocoel or to the surface of the epithelium. Cells outside the embryo sometimes re-enter the epithelium. Some pigment cells at the wound site also disappear. Pigment cells that are inside the larva often degranulate until the cells become almost transparent with very few pigment vesicles. In other cases pigment cells outside the embryo go missing between frames. These are probably swept away by ciliary movements. Once the wound is closed a number of pigment cells remain in the vicinity at least for the duration of the movies (about 2 hrs) and their movement slows to approximate the pre-injury level.

Blastocoelar cells engage in wound repair in a manner entirely different from the pigment cells, and we assume they also participate in pathogen destruction. Some blastocoelar cells arrive at the site of a penetrated skeletal element and move outside the embryo, extend lamellipodia and dynamically move around the skeleton (Fig. 6). Often, as seen in the movies, this behavior is followed by excision of the skeletal element at that site, thereby allowing the epithelium to seal the wound. A single cell RNA-seq analysis of the early cell lineages indicates that blastocoelar cells express a number of proteases at the time the excision occurs and these could degrade the skeletal matrix proteins (Massri et al., 2021), but to date we don’t know which enzymes might be active in the process. The albino embryo experiment showed that skeletal tips were removed in the absence of pigment cells indicating that a distinct cell type was responsible. Also, some of the movies showed a natural phenomenon. The number of pigment cells in larvae is variable and some larvae are almost devoid of pigment cells. Several movies of wound repair in poorly pigmented larvae also showed skeletal excision in arms that were devoid of pigment cells. When we knocked down expression of *irf4*, a transcription factor necessary for blastocoel cell specification, we failed to see cases of skeletal remodeling following a skeletal penetration of the epithelium. Together, these data support the conclusion that the blastocoelar cells are the cells equipped to conduct the skeletal remodeling activity.

Much remains to be discovered about this immune response and repair of the epithelium following a wound. There appears to be a signal of some sort that attracts the pigment cells and likely the blastocoelar cells to the wound site. In vertebrate innate immune responses, a number of cytokines have been identified. While a survey of annotated genes in the sea urchin genome reveals the presence of a number of cytokine-like signals as candidates (Hibino et al., 2006), the identity of those involved in the observed wound response has yet to be known. The impressive number of Toll-like receptors in the sea urchin genome could also be involved (Hibino et al., 2006) providing some specificity that might explain why some but not all pigment cells respond to a given wound. Also, cAMP has been reported to be released by pigment cells and when that release is inhibited, gastrulation is affected (Shipp et al., 2015). Whether cAMP is used as a migratory signal by pigment cells to attract other pigment cells isn’t known, but cAMP is well known as an attraction signal in *Dictyostelium* (Konijn et al., 1967; Firtel et al., 1989).

The blastocoelar cells in excising the skeleton act in a way similar to vertebrate osteoclasts which, although part of bone physiology, originate from the hematopoietic cell lineage. Osteoclasts have been shown to respond to cytokines in rheumatoid arthritis in order to remodel bone (Choy, 2012). Whether there is an evolutionary relationship between the blastocoelar cells and osteoclasts remains unknown though both have a function in remodeling biomineral skeletons. Normally many of the blastocoelar cells reside in or on the biomatrix surrounding the growing skeleton of the sea urchin, and in vertebrates, osteoclasts are found in the matrix surrounding the bone. At present it isn't known whether this class of blastocoelar cells also performs a remodeling function as part of skeletal patterning mechanisms in sea urchin development.

While these and many other questions remain unanswered, the larvae have an immune system capable of protecting them during that stage of their life history. Pigment cells and blastocoelar cells provide that immune response, and their very presence suggests that in evolution, there has been a selective advantage for a larva to have a vigorous wound response for the species to survive while in the water column. And since the sea urchin is a basal deuterostome this response also offers the possibility of gaining a better understanding of how the vertebrate hematopoietic cell lineage diversified to offer both innate and adaptive immune responses.

Materials and Methods

Animals.

Adult *Lytechinus variagatus* animals were obtained from either the Duke Marine Laboratory or from the Pelagic Corp., Florida. Gametes were obtained by injection of 0.5M KCl. Embryos were cultured at 23°C in artificial sea water.

Culture conditions.

Cultures contained low concentrations of embryos in artificial sea water (ASW). No antibiotics were used. Starting cultures contained about 10^5 bacteria per ml with the bacteria introduced by the eggs that were washed once in ASW before being fertilized and twice after fertilization. The pathological experiment added bacteria from bald sea urchin diseased regions to a final concentration of about 3×10^6 bacteria per ml. Bacteria from these diseased regions were isolated and 16s RNA sequenced to identify probable species. Two species of Vibrio identified as V. alginolyticus and V. tubiaschi were identified. We did not further identify the most highly pathogenic species so we refer to the pathogenic bacterium as Vibrio sp.

Mechanical bioassay to assess larval wound response and repair.

Short exposure to 2X seawater (15 sec) removes cilia from the larvae without damaging the embryo. The immobilized larvae are mounted between a protamine sulfate coated slide and coverslip separated by bits of plasticene at the corners of the coverslip (George and McClay, 2019). Pressure is applied to the coverslip while viewing the larvae under a dissecting microscope. A wound is introduced when the pressure is observed to slightly compress the larva. The pressure is then released and the slide sealed with VALAP, mounted on a

compound microscope, and imaged by time-lapse at intervals of 30 sec for two hours or as long as the larvae remain in place. Movies collected include Z-sections allowing us to follow cells over time in 3 dimensions as they move to different focus levels. Processing and tracking cells used ImageJ. Pigment cells are tracked manually using Mtrack (Meijering et al., 2012). Some movie sequences for this project were obtained using fluorescence microscopy of embryos in which one blastomere was injected with FITC at the 2- or 4-cell stage, or with mRNA expressing *gfp* attached to a transmembrane sequence (Saunders and McClay, 2014). Images and movies were obtained on a Zeiss Axio Imager M2 microscope using Zen software and postprocessing using ImageJ. Images were collected either using a 20X or 40X objective (George and McClay, 2019).

Laser cut bioassay

Eggs were injected with Calcein Green Dextran (CGD) A stock solution of 5 mg/ml in dist. Water was injected to about 1% of the total egg volume (Covian-Nares et al., 2010). Two to three-day larvae were deciliated as above and mounted on protamine sulfate coated slides and sealed with VALAP to prevent dehydration (George and McClay, 2019). Care was taken to prevent these larvae from accidental injury. The slide was mounted on a Zeiss Axio Imager microscope equipped with a laser microbeam that was used to make defined laser cuts in the larval epithelium (Kiehart et al., 2006; Wells et al., 2014). The cut and subsequent changes were imaged by fluorescent illumination at 40X with a 1.2 NA water immersion objective. Prior to the laser cut we focused on a relatively flat surface of the dorsal ectoderm, in the plane of that epithelium. The lights were extinguished, and the microscope switched to a high speed camera capable of imaging low fluorescent light levels. The laser microbeam cut along a pre-defined path for 2 sec. Sequences before, during and after the laser cut were collected at 0.09s/frame for 1000 frames or 1.5 min per movie before switching to time lapse conditions.

In situ analysis.

Digoxigenin (DIG) or Fluorescein (FLU) RNA probes were synthesized *in vitro* with a T7 or Sp6 RNA polymerase. Embryos were fixed in 4% paraformaldehyde in artificial sea water (McClay et al., 2020; Slota and McClay, 2018). Probes used in this analysis were *pks1, sult* (Calestani et al., 2003) and *irf4* (Hibino et al., 2006).

Drug treatments.

Larvae were added to SW plus verapamil (50μM; EMD Millipore Corp.) 30 min before introduction of a wound either by compression or by laser. The working concentration matched concentrations used for previous experiments with the sea urchin (Nakajima and Burke, 1996; Yasumasu et al., 1985). Embryos washed out of the drug continued to develop normally. That concentration had little effect on blastocoelar cell movements, nor did it affect the muscle contractions used in larval swallowing.

Morpholino and membrane-GFP microinjections.

Morpholinos to *gcm* (GCTTTGGGCTTTTCTTTTGCACCAT, 500μM) and *irf4* (TTTTGTTATGGGACATCATCACG, 750μM), were injected into eggs. The morpholinos

(Gene Tools Inc.) were dissolved in 100 μl of molecular grade water. They were diluted to working concentrations in FITC and glycerol. Membrane-GFP was synthesized and injected into embryos at the 2 and 4-cell stage (Saunders and McClay, 2014; von Dassow et al., 2019).

Supplementary Material

Refer to Web version on PubMed Central for supplementary material.

Acknowledgements:

We thank the McClay and Wray labs for input on this paper. We than Dr. Lindsay Saunders and her undergraduate microbiology class for culturing and identifying the bacteria from the diseased sea urchin tests. This project was initiated by Taji Phillips, an undergraduate who obtained preliminary data that led to this analysis.

Funding:

Support was provided by NIH RO1 HD14483 (to DRM), NIH T32HD040372 (to RLA), an NSF predoctoral fellowship GRFP 1644868 (to RLA), and NIH NIGMS R35127059 (to DPK).

References

Becker PT, Egea E, Eeckhaut I, 2008. Characterization of the bacterial communities associated with the bald sea urchin disease of the echinoid Paracentrotus lividus. J Invertebr Pathol 98, 136–147. [PubMed: 18191940]

Biswas PS, Bhagat G, Pernis AB, 2010. IRF4 and its regulators: evolving insights into the pathogenesis of inflammatory arthritis? Immunol Rev 233, 79–96. [PubMed: 20192994]

Bollig N, Brustle A, Kellner K, Ackermann W, Abass E, Raifer H, Camara B, Brendel C, Giel G, Bothur E, Huber M, Paul C, Elli A, Kroczek RA, Nurieva R, Dong C, Jacob R, Mak TW, Lohoff M, 2012. Transcription factor IRF4 determines germinal center formation through follicular T-helper cell differentiation. Proc Natl Acad Sci U S A 109, 8664–8669. [PubMed: 22552227]

Buckley KM, Ho ECH, Hibino T, Schrankel CS, Schuh NW, Wang G, Rast JP, 2017. IL17 factors are early regulators in the gut epithelium during inflammatory response to Vibrio in the sea urchin larva. Elife 6.

Buckley KM, Rast JP, 2012. Dynamic evolution of toll-like receptor multigene families in echinoderms. Front Immunol 3, 136. [PubMed: 22679446]

Buckley KM, Rast JP, 2015. Diversity of animal immune receptors and the origins of recognition complexity in the deuterostomes. Dev Comp Immunol 49, 179–189. [PubMed: 25450907]

Buckley KM, Rast JP, 2019. Immune activity at the gut epithelium in the larval sea urchin. Cell Tissue Res 377, 469–474. [PubMed: 31463705]

Buckley KM, Schuh NW, Heyland A, Rast JP, 2019. Analysis of immune response in the sea urchin larva. Methods Cell Biol 150, 333–355. [PubMed: 30777183]

Calestani C, Rast JP, Davidson EH, 2003. Isolation of pigment cell specific genes in the sea urchin embryo by differential macroarray screening. Development 130, 4587–4596. [PubMed: 12925586]

Calestani C, Wessel GM, 2018. These Colors Don't Run: Regulation of Pigment-Biosynthesis in Echinoderms. Results Probl Cell Differ 65, 515–525. [PubMed: 30083933]

Ch Ho E, Buckley KM, Schrankel CS, Schuh NW, Hibino T, Solek CM, Bae K, Wang G, Rast JP, 2016. Perturbation of gut bacteria induces a coordinated cellular immune response in the purple sea urchin larva. Immunol Cell Biol 94, 861–874. [PubMed: 27192936]

Choy E, 2012. Understanding the dynamics: pathways involved in the pathogenesis of rheumatoid arthritis. Rheumatology (Oxford) 51 Suppl 5, v3–11. [PubMed: 22718924]

Coates CJ, McCulloch C, Betts J, Whalley T, 2018. Echinochrome A Release by Red Spherule Cells Is an Iron-Withholding Strategy of Sea Urchin Innate Immunity. J Innate Immun 10, 119–130. [PubMed: 29212075]

Covian-Nares JF, Koushik SV, Puhl HL 3rd, Vogel SS, 2010. Membrane wounding triggers ATP release and dysferlin-mediated intercellular calcium signaling. J Cell Sci 123, 1884–1893. [PubMed: 20442251]

Duboc V, Lapraz F, Saudemont A, Bessodes N, Mekpoh F, Haillot E, Quirin M, Lepage T, 2010. Nodal and BMP2/4 pattern the mesoderm and endoderm during development of the sea urchin embryo. Development 137, 223–235. [PubMed: 20040489]

Eisen A, Kiehart DP, Wieland SJ, Reynolds GT, 1984. Temporal sequence and spatial distribution of early events of fertilization in single sea urchin eggs. J Cell Biol 99, 1647–1654. [PubMed: 6490715]

Fedoreyev SA, Krylova NV, Mishchenko NP, Vasileva EA, Pislyagin EA, Iunikhina OV, Lavrov VF, Svitich OA, Ebralidze LK, Leonova GN, 2018. Antiviral and Antioxidant Properties of Echinochrome A. Mar Drugs 16.

Firtel RA, van Haastert PJ, Kimmel AR, Devreotes PN, 1989. G protein linked signal transduction pathways in development: dictyostelium as an experimental system. Cell 58, 235–239. [PubMed: 2546676]

Flutter B, Nestle FO, 2013. What on “irf” is this gene 4? Irf4 transcription-factor-dependent dendritic cells are required for T helper 2 cell responses in murine skin. Immunity 39, 625–627. [PubMed: 24138876]

George AN, McClay DR, 2019. Methods for transplantation of sea urchin blastomeres. Methods Cell Biol 150, 223–233. [PubMed: 30777177]

Gibson AW, Burke RD, 1985. The origin of pigment cells in embryos of the sea urchin *Strongylocentrotus purpuratus*. Developmental Biology 107, 414–419. [PubMed: 3972163]

Gordon S, 2016. Elie Metchnikoff, the Man and the Myth. J Innate Immun 8, 223–227. [PubMed: 26836137]

Gustafson T, Kinnander H, 1956. Microaquaria for time-lapse cinematographic studies of morphogenesis of swimming larvae and observations on gastrulation. . Exp. Cell Res. 11 36–57. [PubMed: 13356825]

Hibino T, Loza-Coll M, Messier C, Majeske AJ, Cohen AH, Terwilliger DP, Buckley KM, Brockton V, Nair SV, Berney K, Fugmann SD, Anderson MK, Pancer Z, Cameron RA, Smith LC, Rast JP, 2006. The immune gene repertoire encoded in the purple sea urchin genome. Dev Biol 300, 349–365. [PubMed: 17027739]

Jaffe LF, 1991. The path of calcium in cytosolic calcium oscillations: a unifying hypothesis. Proc Natl Acad Sci U S A 88, 9883–9887. [PubMed: 1946414]

Jaffe LF, Creton R, 1998. On the conservation of calcium wave speeds. Cell Calcium 24, 1–8. [PubMed: 9793683]

Kiehart DP, Tokutake Y, Chang M-S, Hutson MS, Wiemann JM, Peralta X, Toyama Y, A.R. W., Ridriquez A., Edwards GS., 2006. Ultraviolet laser microbeam for dissection of Drosophila embryos, 3rd ed. Elsevier Academic Press, San Diego, CA.

Kominami T, Takata H, Takaichi M, 2001. Behavior of pigment cells in gastrula-stage embryos of Hemicentrotus pulcherrimus and Scaphechinus mirabilis. Dev Growth Differ 43, 699–707. [PubMed: 11737150]

Konijn TM, Van De Meene JG, Bonner JT, Barkley DS, 1967. The acrasin activity of adenosine-3’,5’-cyclic phosphate. Proc Natl Acad Sci U S A 58, 1152–1154. [PubMed: 4861307]

Krupke OA, Zysk I, Mellott DO, Burke RD, 2016. Eph and Ephrin function in dispersal and epithelial insertion of pigmented immunocytes in sea urchin embryos. Elife 5.

Massri AJ, Greenstreet L, Afanassiev A, Berrio A, Wray GA, Schiebinger G, McClay DR, 2021. Developmental single-cell transcriptomics in the Lytechinus variegatus sea urchin embryo. Development 148.

McClay DR, Warner J, Martik M, Miranda E, Slota L, 2020. Gastrulation in the sea urchin. Curr Top Dev Biol 136, 195–218. [PubMed: 31959288]

Meijering E, Dzyubachyk O, Smal I, 2012. Methods for cell and particle tracking. Methods Enzymol 504, 183–200. [PubMed: 22264535]

Miller J, Fraser SE, McClay D, 1995. Dynamics of thin filopodia during sea urchin gastrulation. Development 121, 2501–2511. [PubMed: 7671814]

Nakajima Y, Burke RD, 1996. The initial phase of gastrulation in sea urchins is accompanied by the formation of bottle cells. Developmental Biology 179, 436–446. [PubMed: 8903358]

Pohl JM, Gutweiler S, Thiebes S, Volke JK, Klein-Hitpass L, Zwanziger D, Gunzer M, Jung S, Agace WW, Kurts C, Engel DR, 2017. Irf4-dependent CD103(+)CD11b(+) dendritic cells and the intestinal microbiome regulate monocyte and macrophage activation and intestinal peristalsis in postoperative ileus. Gut 66, 2110–2120. [PubMed: 28615301]

Ransick A, Davidson EH, 2006. cis-regulatory processing of Notch signaling input to the sea urchin glial cells missing gene during mesoderm specification. Dev Biol 297, 587–602. [PubMed: 16925988]

Ransick A, Davidson EH, 2012. Cis-regulatory logic driving glial cells missing: self-sustaining circuitry in later embryogenesis. Dev Biol 364, 259–267. [PubMed: 22509525]

Rast JP, Smith LC, Loza-Coll M, Hibino T, Litman GW, 2006. Genomic insights into the immune system of the sea urchin. Science 314, 952–956. [PubMed: 17095692]

Saunders LR, McClay DR, 2014. Sub-circuits of a gene regulatory network control a developmental epithelial-mesenchymal transition. Development 141, 1503–1513. [PubMed: 24598159]

Service M, Wardlaw AC, 1984. Echinochrome-a as a Bactericidal Substance in the Celomic Fluid of Echinus-Esculentus (L). Comp Biochem Phys B 79, 161–165.

Sherwood DR, McClay DR, 1997. Identification and localization of a sea urchin Notch homologue: insights into vegetal plate regionalization and Notch receptor regulation. Development 124, 3363–3374. [PubMed: 9310331]

Sherwood DR, McClay DR, 1999. LvNotch signaling mediates secondary mesenchyme specification in the sea urchin embryo. Development 126, 1703–1713. [PubMed: 10079232]

Shipp LE, Hill RZ, Moy GW, Gokirmak T, Hamdoun A, 2015. ABCC5 is required for cAMP-mediated hindgut invagination in sea urchin embryos. Development 142, 3537–3548. [PubMed: 26395488]

Slota LA, McClay DR, 2018. Identification of neural transcription factors required for the differentiation of three neuronal subtypes in the sea urchin embryo. Dev Biol 435, 138–149. [PubMed: 29331498]

Smith LC, Ghosh J, Buckley KM, Clow LA, Dheilly NM, Haug T, Henson JH, Li C, Lun CM, Majeske AJ, Matranga V, Nair SV, Rast JP, Raftos DA, Roth M, Sacchi S, Schrankel CS, Stensvag K, 2010. Echinoderm immunity. Adv Exp Med Biol 708, 260–301. [PubMed: 21528703]

Sweet HC, Gehring M, Ettensohn CA, 2002. LvDelta is a mesoderm-inducing signal in the sea urchin embryo and can endow blastomeres with organizer-like properties. Development 129, 1945–1955. [PubMed: 11934860]

Tamboline CR, Burke RD, 1992. Secondary mesenchyme of the sea urchin embryo: ontogeny of blastocoelar cells. J Exp Zool 262, 51–60. [PubMed: 1583452]

Tussiwand R, Lee WL, Murphy TL, Mashayekhi M, Kc W, Albring JC, Satpathy AT, Rotondo JA, Edelson BT, Kretzer NM, Wu X, Weiss LA, Glasmacher E, Li P, Liao W, Behnke M, Lam SS, Aurthur CT, Leonard WJ, Singh H, Stallings CL, Sibley LD, Schreiber RD, Murphy KM, 2012. Compensatory dendritic cell development mediated by BATF-IRF interactions. Nature 490, 502–507. [PubMed: 22992524]

von Dassow G, Valley J, Robbins K, 2019. Microinjection of oocytes and embryos with synthetic mRNA encoding molecular probes. Methods Cell Biol 150, 189–222. [PubMed: 30777176]

Wells AR, Zou RS, Tulu US, Sokolow AC, Crawford JM, Edwards GS, Kiehart DP, 2014. Complete canthi removal reveals that forces from the amnioserosa alone are sufficient to drive dorsal closure in Drosophila. Mol Biol Cell 25, 3552–3568. [PubMed: 25253724]

Williams JW, Tjota MY, Clay BS, Vander Lugt B, Bandukwala HS, Hrusch CL, Decker DC, Blaine KM, Fixsen BR, Singh H, Sciammas R, Sperling AI, 2013. Transcription factor IRF4 drives dendritic cells to promote Th2 differentiation. Nat Commun 4, 2990. [PubMed: 24356538]

Yasumasu I, Mitsunaga K, Fujino Y, 1985. Mechanism for electrosilent Ca2+ transport to cause calcification of spicules in sea urchin embryos. Exp Cell Res 159, 80–90. [PubMed: 4029269]

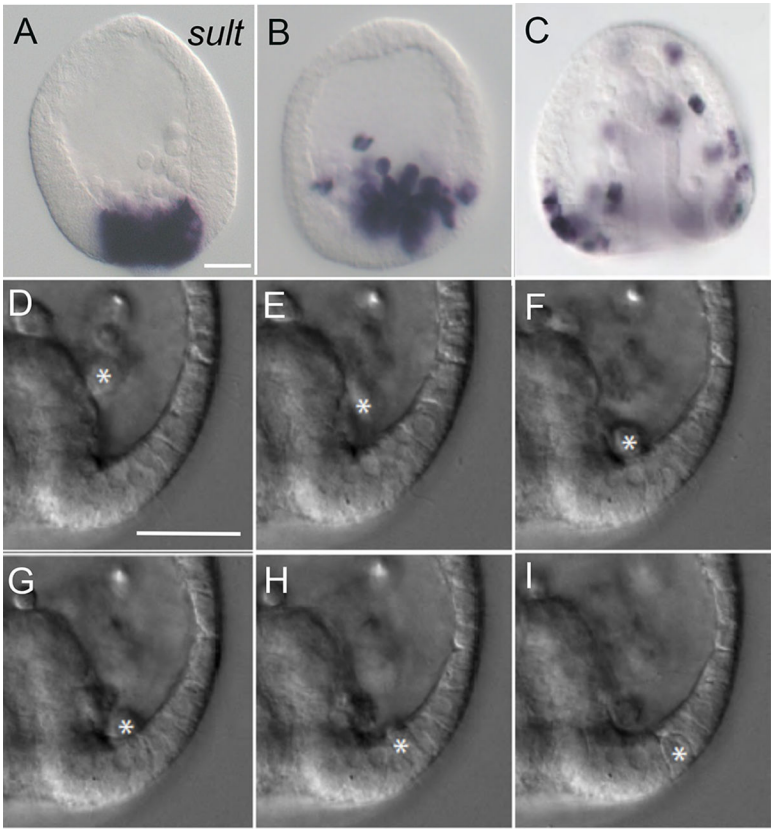

Fig. 1. Pigment cells ingress and move to the dorsal ectoderm.

A-C. Pigment cell progenitors imaged by in situ hybridization of *sult* (Calestani et al., 2003) at the mesenchyme blastula stage (**A**), early gastrula (**B**), and late gastrula stage (**C**). Pigment cell progenitors enter the blastocoel at the beginning of the gastrula stage and move to the posterior blastocoel where many of them enter the ectoderm. They then migrate both within the ectoderm and along the lining of the dorsal blastocoel to distribute the population throughout the dorsal ectoderm and its basement membrane. **D-I.** Images from a time-lapse movie at early gastrula showing a pigment progenitor cell (asterisk) migrating posteriorly, and entering the ectoderm. Bar A-C = 25 μm, D-I = 25 μm.

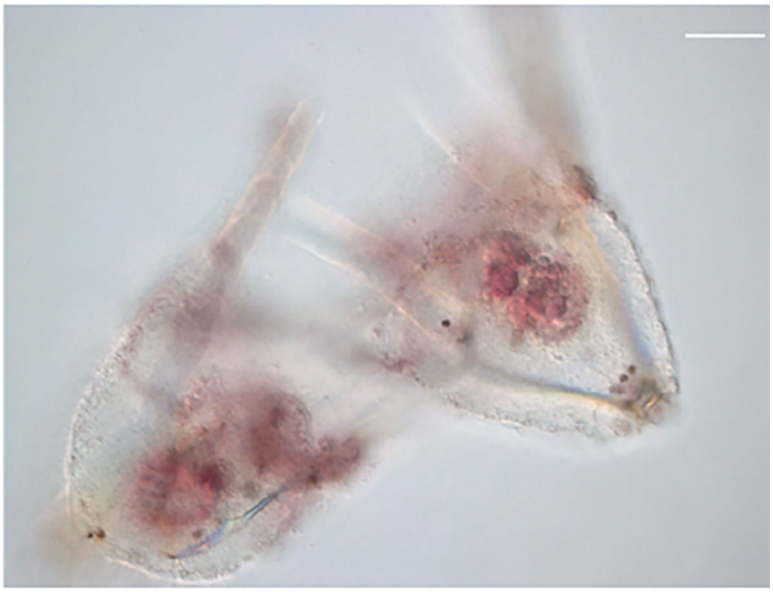

Fig. 2. Pigment cell response to an pathogenic infection.

Image of two larva 24 hrs after infecting the culture with Vibrio sp. Most pigment cells have entirely degranulated after turning black. A few black pigment cells remain in each of the larvae. The gut is stained red from release of echinochrome A. Bar = 20μm.

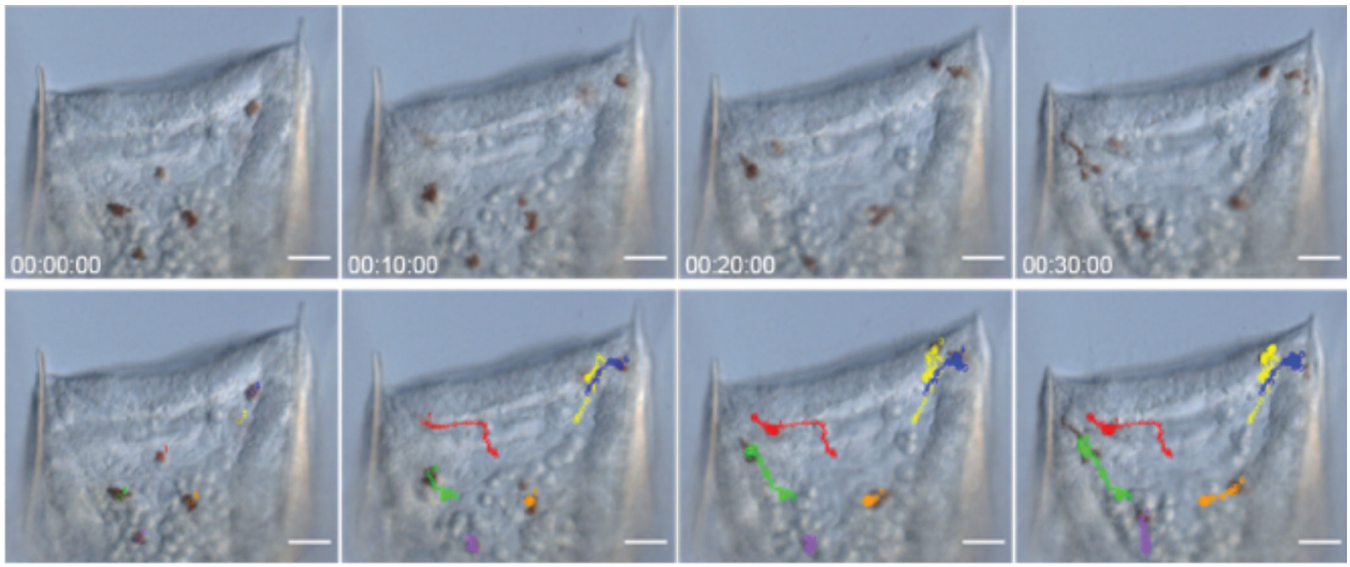

Fig. 3. Tracking and quantification of pigment cell movements.

Six pigment cells are tracked during the migration to either of two wound sites in the oral hood of the larva where skeletal tips penetrate the epithelium. The images are taken from a time lapse movie at intervals of 10 min. A single focal plane is shown in each image though the pigment cells were tracked through the Z-plane as they migrated. Bar = 20 μm.

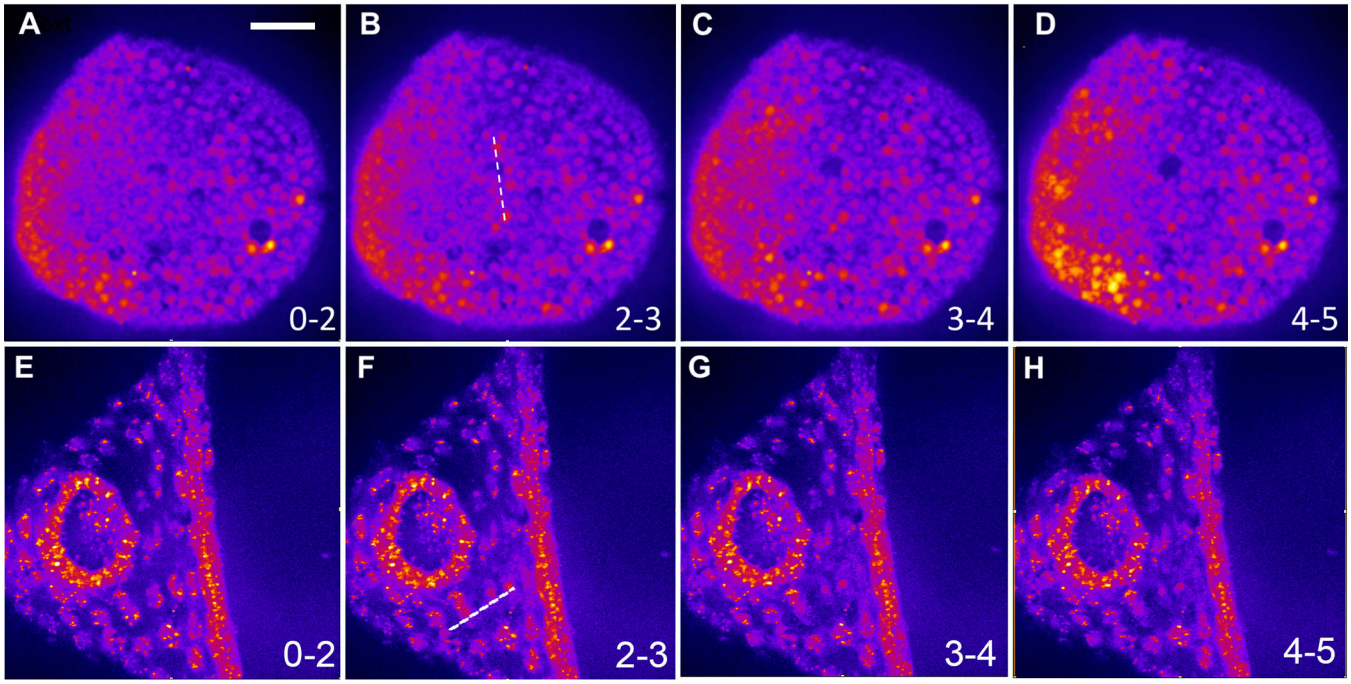

Fig. 4. A calcium transient rapidly spreads across the embryo.

(A-D) Heatmaps of four frames from Movie S7 were captured. Frame A shows a plane of larval epithelium prior to the laser cut. Frame B shows the location of the cut (dashed line) which was made between seconds 2–3. Cells at that site exhibit calcium release as seen by an increase in fluorescence, or increased red in this pseudocolored image. Frames C and D show the same epithelial sheet one and two seconds later. Comparison of images show progress of the calcium wave as it emanates from the site of the laser cut. (**E-H)** Four frames from a Verapamil treated larva. Dashed line in F. shows the location of the laser cut. **G** and **H** show no change in fluorescence in the seconds after the cut. This larva was cut on the dorsal posterior surface. The ring is the gut and the line to the right the ciliary band. Both colored more strongly in this heatmap because of multiple cell layers in the Z plane. The images were stacked and the Z planes projected at maximum intensity. The stacks were pseudocolored in ImageJ with “Fire” to provide a heatmap of the calcium-induced fluorescence with blue being low fluorescence and red to white indicating stronger fluorescent signals. Bar = 25 μm.

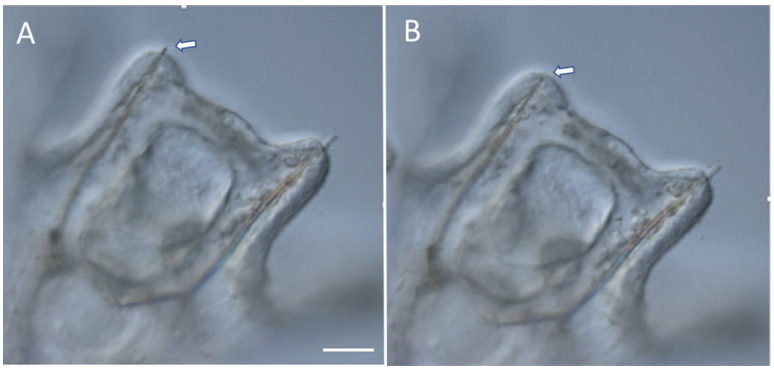

Fig. 5. Skeletal tips break without pigment cells.

A. Image from an albino embryo in movie S8 showing a skeletal tip penetrating through the epidermis. **B.** Image from the same movie after the skeletal tip is broken off in the absence of pigment cells. The skeletal tip on the right side was not excised during the movie. Bar = 25 μm.

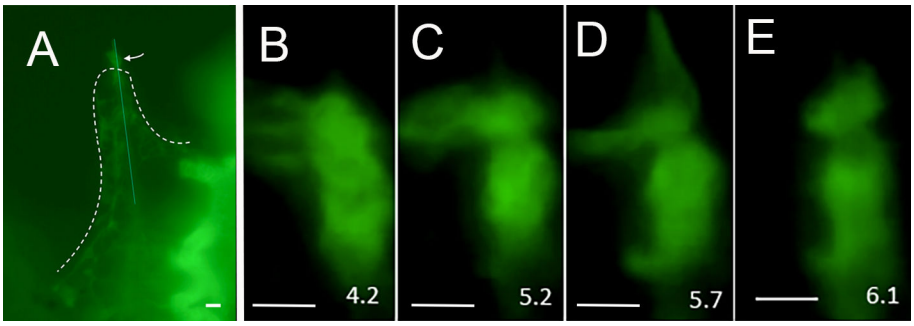

Fig. 6. Blastocoelar cells dynamically wrap around protruding skeletal tips.

A. Screen shot of the ½ GFP-labeled larva imaged in movie S9. The GFP half is to the right and the unlabeled portion of the larvae to the left. The dotted line outlines an unlabeled arm of the oral hood. A thin blue line traces the skeleton on that side including its penetration to the outside of the embryo. The white arrow points to a blastocoelar cell, labeled with GFP, therefore originating from the labeled half of the embryo. **B-E.** are magnified images of that same blastocoelar cell captured at the time points in movie S9 at the times indicated (min). The Images show some of the active extensions of lamellapodia by the blastocoelar cell that is wrapped around a skeletal tip. Bar = 5μm.

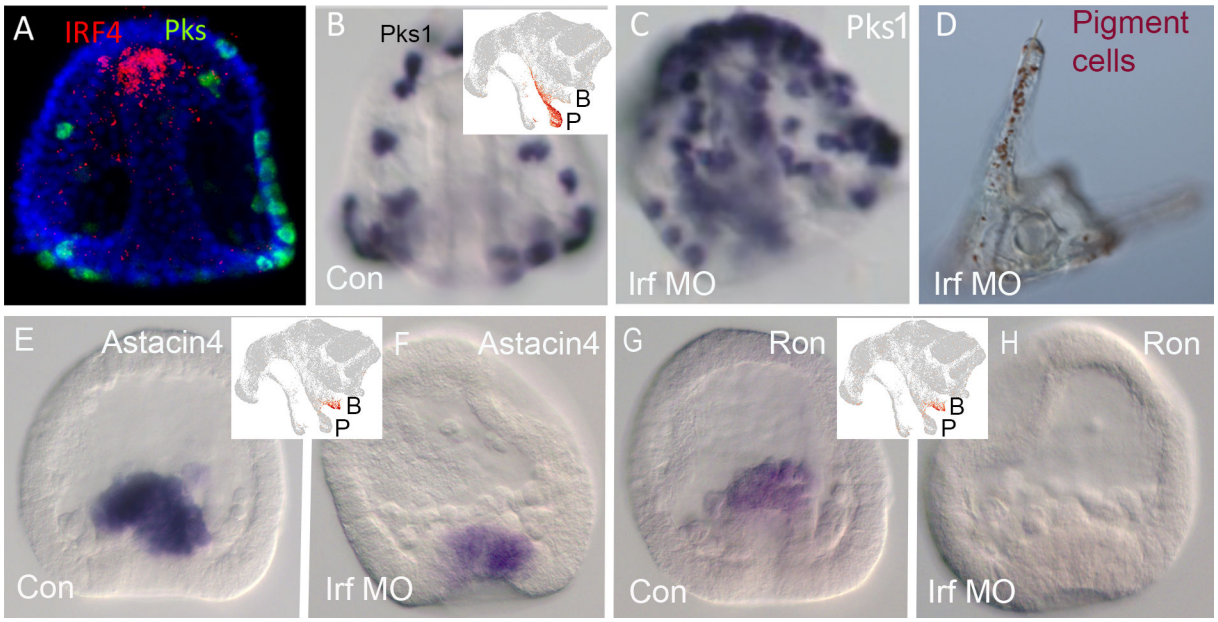

Fig. 7. Irf4 knockdown produces excess pigment cells.

A. A double *in situ* showing pigment cells expressing *pks1* and blastocoelar cells expressing *irf4* at the tip of the archenteron at late gastrula stage. **B.** *In* situ of Pigment cells at late gastrula stage in control embryos. **C.** *In situ* of *pks1*-expressing pigment cells at late gastrula stage in *irf4*-morpholino knockdown embryos. **D.** An *irf4* knockdown larval arm contains an excess number of pigment cells. Insert in **B** shows a UMAP from a temporal scRNA-seq analysis (Massri et al., 2021). The strongest expression of Pks1 appears in the lineage leading to pigment cells (P). The branch leading to (B) is the blastocoelar lineage. Inserts within **E, F** and **G, H** show that Astacin4 and Ron are genes expressed exclusively in the Blastocoelar lineage. Knockdowns of *irf4* reduces or eliminates expression of *astacin4* and *ron* (**F** and **H**). UMAP inserts show the localized expression of these two genes in the blastocoelar lineage. Bar = 25 μm.